Microsatellite-based quantification method to estimate biomass of endophytic Phialocephala species in strain mixtures

Author(s):
Reininger, Vanessa; Grünig, Christoph R.; Sieber, Thomas Niklaus

Publication date:
2011

Permanent link:
https://doi.org/10.3929/ethz-b-000029862

Originally published in:
Microbial Ecology 61(3), https://doi.org/10.1007/s00248-010-9798-z

Microb Ecol (2011) 61:676–683
DOI 10.1007/s00248-010-9798-z

METHODS

Microsatellite-Based Quantification Method to Estimate Biomass of Endophytic *Phialocephala* Species in Strain Mixtures

Vanessa Reininger · Christoph R. Grünig · Thomas N. Sieber

Received: 1 October 2010 / Accepted: 20 December 2010 / Published online: 22 January 2011

Abstract Fungi of the *Phialocephala fortinii* sensu lato–*Acephala applanata* species complex (PAC) are ubiquitous endophytic colonizers of tree roots in which they form genotypically diverse communities. Measurement of the colonization density of each of the fungal colonizers is a prerequisite to study the ecology of these communities. Up to now, there is no method readily available for the quantification of PAC strains co-colonizing the same root. The new DNA quantification method presented here is based on the amplification of microsatellites by competitive polymerase chain reaction (PCR). The method proved to be suitable to detect and quantify at least two strains within one single sample by the addition of a known amount of mycelium of a reference strain before DNA extraction. The method exploits the correlation between the reference/target ratio of light emitted during microsatellite detection (peak ratio) and the reference/target ratio of mycelial weights to determine the biomass of the target strain. Hence, calibration curves were obtained by linear regression of the peak ratios on the weight ratios for different mixtures of reference and target strains. The slopes of the calibration curves and the coefficients of determination were close to 1, indicating that peak ratios are good predictors of weight ratios. Estimates of fungal biomass in mycelial test mixtures of known composition laid within the 95% prediction interval and deviated on average by 16% (maximally 50%) from the true biomass. On average, 3–6% of the root biomass of Norway spruce seedlings consisted of mycelial biomass of either one of two inoculated PAC strains. Biomass estimates obtained by real-time quantitative PCR were correlated with the estimates obtained by the microsatellite-based method, but variation between the two estimates from the same root was high in some samples. The microsatellite-based DNA quantification method described here is currently the best method for strainwise estimation of endophytic biomass of PAC fungi in small root samples.

Electronic supplementary material The online version of this article (doi:10.1007/s00248-010-9798-z) contains supplementary material, which is available to authorized users.

V. Reininger (✉) · C. R. Grünig · T. N. Sieber
Institute of Integrative Biology, Forest Pathology and Dendrology, ETH Zurich,
Universitätstrasse 16,
8092 Zürich, Switzerland
e-mail: vanessa.reininger@env.ethz.ch

Introduction

Pathogenic and beneficial microorganisms are essential forces shaping plant communities. In addition to mycorrhizal fungi, plants are associated with fungal endophytes, which can occupy different niches from the roots to the needles or leaves [26, 27]. Symbiotic relationships between endophytes and plants exist on a continuum from mutualism to antagonism [19]. Mutualistic relationships can change into antagonistic ones and vice versa if conditions change [19]. Switching endophyte behavior from one type of relationship to another depends on the predisposition of the host tissue, environmental factors, and the extent of colonization. It has been postulated that plant tissues die as soon as the endophyte's density of colonization exceeds a certain threshold value [22].

Dark septate endophytes (DSE) [23] are ubiquitous fungal colonizers of apparently healthy plant roots [1, 6, 10–12, 18, 20, 24]. *Phialocephala fortinii* sensu lato, which comprises several reproductively isolated cryptic species [8, 9], and the closely related *Acephala applanata* were identified as the major components of DSE communities

in tree roots. Members of the *P. fortinii* s.l.–*A. applanata* species complex (PAC) occur sympatrically, often adjacent to each other or intermingled in the same root segment where they compete for space and nutrients [9, 21]. In forest ecosystems, communities of PAC form persistent complex networks [14]. PAC can behave as commensals, mutualists, or opportunistic pathogens depending on genetic traits and environment and may affect plant performance and plant communities' composition [9]. Understanding the mechanisms shaping PAC communities is important for the interpretation of ecosystem responses to environmental change. We hypothesize that inter- and intraspecific competition among PAC strains is a key factor in community dynamics of these dominant root colonizers.

However, testing this hypothesis requires proper measurement of biomass of co-occurring PAC strains. Several methods were described allowing to quantify the extent of microbial colonization in host tissues such as real-time quantitative polymerase chain reaction (PCR) [2], competitive PCRs [30] or pyrosequencing [3, 25]. A real-time quantitative PCR assay specific for PAC species was developed recently [28]. However, the quantification of conspecific individuals or of closely related species by PCR-based quantification methods is complicated by the low level of DNA polymorphisms. For example, sequences of several coding and non-coding genomic loci of PAC were identical on the intraspecies and even on the interspecies level [16, 29]. In contrast, pronounced length differences were observed in microsatellites at the intra- and interspecies level of PAC.

The new DNA quantification method presented here is based on the amplification of microsatellites by competitive PCR, which is a very precise quantification tool [30]. The amplicons are separated by capillary electrophoresis and detected fluorometrically. Retention times differ among strains due to strain specific allele lengths. Consequently, the light emission peak of each strain appears at a different position on the fluorogram making detection of each strain possible. The area under the peak is proportional to the DNA amount in the original sample. This area-under-the-peak ratio, called "peak ratio" hereafter, from reference to target strain is proportional to the biomass ratio of these two strains, allowing estimation of biomass of the target strain.

Naef et al. [13] successfully estimated biomass of single fungal strains by microsatellite-based competitive PCR. We extended the "dual" system of Naef et al. [13] to a "triple" system. This allows biomass estimation of two strains of the same or different species co-occurring in one sample by the addition of a known amount of mycelium of a third strain. We tested the "triple" system using roots of *Picea abies* (Norway spruce) seedlings colonized simultaneously by two PAC strains comparing endophyte biomass estimates obtained by the newly developed microsatellite-based quantification method with those obtained by real-time quantitative PCR.

Methods

Fungal Strains, Culture Conditions, and Mycelium Mixtures Used for Calibration

Multiplex and singleplex PCR for the amplification of microsatellites of PAC has been developed recently, and allele data are available for more than 5,000 PAC strains [16]. Several highly polymorphic microsatellite loci are known, allowing discrimination of many PAC strains within and among PAC species. Suitability of four loci (mPF_043, mPF_049, mPF_142B, and mPF_860B) for DNA quantification was tested initially [16], but only locus mPF_142B was developed further because this locus produced fewest stutter bands. Four PAC strains with different alleles at microsatellite locus mPF_142B [15] were chosen to develop the "triple" system (Table 1). Strains were cultivated for 2 weeks in 100-ml Erlenmeyer flasks containing 50 ml malt broth (15 g l^{-1} malt extract) on a shaker at 20°C and 80 rpm. The mycelium was harvested and lyophilized. The freeze-dried mycelium of each of two target strains (target strains 1 and 2) was mixed according to the weight ratios (m_1/m_2) 1:14, 3:12, 5:10, 7:8, 9:6, 11:4, 13:2, and 14:1, and a constant amount of 15 mg mycelium (m_r) of a third strain (reference strain) was added. The total weight of all three strains was kept constant at 30 mg. Mycelial mixtures were homogenized and DNA extracted as described previously [7].

Amplification of Microsatellites by Competitive PCR

Locus mPF_142B was amplified by PCR according to Queloz et al. [15] in 15 µl volumes containing 2 µl 1:50 or 1:500 diluted DNA, 50 mM KCl, 10 mM Tris–HCl, 1.5 mM $MgCl_2$, 200 µM dNTPs (Amersham Pharmacia Biotech), 0.4 µM of each primer (F, GCTTTCACATCAC-CATCCAG; R, GGTGAGTTGGTTGCGAGTTT) and 0.3 U Taq polymerase (Amersham Pharmacia Biotech). The running conditions were 2 min at 94°C followed by 36 cycles of denaturation for 30 s at 94°C, annealing for 30 s at 53°C, and extension for 30 s at 72°C (followed by a final extension step of 10 min at 72°C).

Microsatellite Fragment Analysis

Fifteen-fold diluted triplicates were prepared from each PCR reaction: 4 µl of the dilutions were mixed with 9.05 µl Hi-Di™ formamide and 0.25 µl GeneScan™ 500 LIZ™ (Applied Biosystems). Fragment lengths and the peak area, i.e., the amount of PCR product, of each fragment, were measured using an ABI 3730xl DNA analyser (Applied Biosystems) and analyzed using the GeneMapper v. 4.0 software (Applied Biosystems) [16].

Table 1 PAC strains included in this study

ETH-strain number[a]	Strain label	Species	Host	Allele length at locus mPF_142B (bp)
6_2_7v[b]	A	*Phialocephala subalpina*	*Vaccinium myrtillus*	174
6_37_6v[b]	B	*Phialocephala subalpina*	*Vaccinium myrtillus*	162
7_45_5[b]	C	*Phialocephala fortinii* s.s.	*Picea abies*	154
7_63_4	D	*Phialocephala fortinii* s.s.	*Picea abies*	152

[a] Fungus culture collection of ETH Zurich, Institute of Integrative Biology, Section Forest Pathology & Dendrology, Zurich, Switzerland

[b] Strain used to test the method with mycelial mixtures

The mycelial weight ratios (m_r/m_1 and m_r/m_2) and the corresponding peak ratios of the amount of the PCR products (p_r/p_1 and p_r/p_2) were determined for each combination of strains. Two multiple linear regressions were performed per strain combination (full models). One of the regressions served to estimate the coefficients β_i considering strain 1 (m_1) to be quantified (target strain) and strain 2 as "additional" strain (m_2), i.e.:

$$(p_r/p_1) = \beta_0 + \beta_1{}^*(m_r/m_1) + \beta_2{}^*(m_r/m_2). \quad (1)$$

The other regression served to estimate the coefficients β_i considering strain 2 (m_2) to be quantified and strain 1 as "additional" strain (m_1), i.e.:

$$(p_r/p_2) = \beta_0 + \beta_1{}^*(m_r/m_1) + \beta_2{}^*(m_r/m_2). \quad (2)$$

Residual analyses were performed and transformations made as needed. The terms $\beta_2{}^*(m_r/m_2)$ in Eq. 1 and $\beta_1{}^*(m_r/m_1)$ in Eq. 2 were included to test for possible disturbing influences of the additional strain on the amplification of the microsatellite of the target strain during competitive PCR. Ideally, β_2 and β_1 do not deviate significantly from zero (i.e., indicating no disturbing influence) in Eqs. 1 and 2, respectively, reducing the equations to equations of simple regression lines (reduced models):

$$(p_r/p_1) = \beta_0 + \beta_1{}^*(m_r/m_1) \quad (3)$$

and

$$(p_r/p_2) = \beta_0 + \beta_2{}^*(m_r/m_2) \quad (4)$$

which can then be used as calibration curves. The 95% prediction intervals were calculated for each calibration curve. The software R was used for all statistical analyses [17].

Testing the "Triple" System with Mycelial Mixtures

To test the method, freeze-dried mycelia of three strains (A, B, and C) were mixed at weight ratios of approximately 3:8:19 and 1:1:1 in different combinations and a total dry weight of 30 mg. Cultivation and harvest of strains, DNA extraction, PCR, and microsatellite fragment analysis followed the protocols described above. Fungal biomass was estimated using the established calibration curves, and estimates were compared with the true weights by regression analysis.

Testing the "Triple" System with Colonized Norway Spruce Roots

Norway spruce seedlings were grown in 1:1 vermiculite–peat mixtures (*v*/*v*) colonized by PAC according to Tellenbach et al. [28] with the following modifications. Instead of 50-ml Falcon tubes, 100-ml polypropylene tubes (Semadeni, Ostermundingen, Switzerland) were used and the sterile vermiculite–peat was colonized by two simultaneously inoculated PAC strains (Table S1). Norway spruce seedlings were harvested after 4 months of incubation in a phytotron [16 h day (120–140 μEm^{-2} s^{-1})/8 h night, temperature (22°C/15°C), and relative humidity (RH 45%)]. Roots were rinsed free from substrate, and seven 5-mm-long root segments were excised from each of three main roots per seedling. The resulting 21 segments per seedling were pooled, freeze-dried, and weighed. Freeze-dried roots and 3 mg of freeze-dried mycelium of the reference strain, added as internal standard, were mixed and homogenized. DNA was extracted from the homogenate and subjected to competitive microsatellite PCR and, thereafter, to fragment analysis. The biomass was estimated using the calibration curves and results displayed as boxplots [5]. Analysis of variance (ANOVA) was used to test for effects of strains, species, and strain combination on the endophytic biomass of each strain. For comparison, the DNA extracts were subjected to PAC-specific real-time quantitative PCR according to Tellenbach et al. [28] to quantify the whole PAC DNA. Regression analysis and robust line fitting using the LOESS algorithm with α=0.5 [4] were used to compare the mycelial biomass estimates obtained by real-time quantitative PCR and the microsatellite method.

Results

Microsatellite Fragment Analysis, Regression Analyses, and Calibration Curves

Differences between the three replicated measurements of the peak areas were minimal and amounted to maximally 2.5%. Regression of the peak ratios (p_r/p_1 or p_r/p_2) on the two mycelial weight ratios (m_r/m_1 and m_r/m_2) using Eqs. 1

or 2 resulted in no significant influence of the additional strain in 12 of 24 comparisons (Table 2). This allowed reduction to monofactorial models, and thus, coefficients of calibration curves (regression lines) and 95% prediction intervals in two-dimensional space could be determined (Fig. 1). The fit of the models was best when the ratios were ln-transformed. The other 12 combinations were significantly influenced by the additional strain (Table 2). The 12 calibration curves resulting from the regressions with no significant influence of the additional strain (shown in the upper half of Table 2) allowed estimation of mycelial weights of both strains in five of the six possible mixtures of two of the four strains. No estimation was possible for mixtures of strain D and B independently of which of the two strains was the target or additional strain, respectively, because both the target and the additional strain always had a significant influence (see footnote a in the lower half of Table 2). The coefficients of determination (R^2) were close to 1, and 9 out of 12 slopes of the regression lines did not deviate significantly from 1 (Fig. 1; Table 2).

Biomass Estimation of Single Strains in Strain Mixtures

The triple system allowed estimating biomass of each strain in mixtures of two strains accurately. The estimated values deviated on average by 16% from the true ones with a maximum deviation of 50% in one single case. However, the estimated values were all within the 95% prediction interval (Fig. 2).

Quantification of PAC Biomass in Norway Spruce Roots

Fungal biomass could be estimated using an internal standard (reference strain) and the appropriate calibration curve. Fungal biomass was measured in gram mycelial dry weight per gram root dry weight (Table S1). The median mycelial biomass of either one of the two inoculated PAC strains varied between approximately 3% and 6% of the root biomass (Fig. 3). The density of root colonization depended on the species. It was significantly higher for *P. subalpina* strains ($p=0.01054$). In contrast, stimulating or inhibitory effects on endophytic colonization were independent on the combination of strains used for inoculation ($p\geq0.1447$). There was a highly significant relationship between estimates of endophytic fungal biomass obtained by real-time quantitative PCR and those obtained by the microsatellite method (Fig. 4, $p=0.008$). However, deviations between the estimates were high and tended to increase with increasing biomass (Fig. 4). The line fitted using the LOESS algorithm indicates that the linear fit is unreliable at endophytic biomasses exceeding approximately 0.004 g.

Discussion

We were able to develop a precise fungal biomass estimation method using microsatellite-based competitive PCR. In contrast to Naef et al. [13], the method allows to differentiate and estimate endophytic biomass of two fungal strains in the same plant tissue. It is even possible to differentiate biomass of conspecific strains. Quantification of strains within the same species, interacting in plant tissues, is an essential tool to study the complex and diverse community structure of PAC species in ecosystems.

Although accuracy of competitive PCR is assumed to exceed that of any other quantitative PCR procedure, including real-time quantitative PCR [30] (see below), the method has some weaknesses: (a) disturbing influence of the additional strains DNA during competitive PCR due to differences in length and nucleotide composition of the target sequences, (2) non-correlatedness of DNA amount and biomass, and (3) bias induced by a large difference in biomass of reference and target strain.

Preferential amplification of the target locus of one or several strains during competitive PCR can be reduced by the selection of strains that possess alleles of similar length. However, the more similar the allele length, the more difficult the discrimination of the light emission peaks during detection, thus making it more difficult to properly measure the area under the different peaks. The additional strain had a disturbing influence on the amplification of the other two strains in 67% of the samples if the smallest length difference among the alleles of the three strains was only 2 bp (i.e., between strain C and D) compared to only 33% of the samples if the length difference was ≥8 bp. Thus, strains and microsatellite loci must be chosen carefully, and the best trade-off between equal probabilities of getting amplified during competitive PCR and measurability must be sought. A difference of 20 bp between the target and competitor allele is considered to be a good compromise [30], and allele distances between strains should be as equal as possible.

The method described here allows quantification of DNA, but biomass and DNA do not necessarily correlate, since cell sizes differ depending on the strain, cell type, and/or culture conditions. For example, microsclerotial cells are small compared to hyphal cells [6, 20, 28]. Thus, the DNA amount relative to biomass is higher in microsclerotial than in hyphal cells. Therefore, the type and composition of the mycelium must be taken into consideration when interpreting biomass estimates. Ideally, strains used for dual inoculations should either be equally good producers of microsclerotia or not produce them at all to improve comparability of biomass estimates for the two strains. No microsclerotia were observed for our strains either in liquid culture or in root segments. Thus, our strains

Table 2 Parameterization of the calibration curves

Target strain	Reference strain	Additional strain	Model	R^2	Intercept β_0	Slopes		p (slopes=0)		p (slope=1)
						β_1	β_2	β_1	β_2	
Strain combinations without significant influence of the additional strain										
A	B	C	Full	0.9983	0.17897	1.03429	−0.06197	$<2\times10^{-16}$*	0.23893	
A	B	C	Reduced	0.9983	0.23542	1.003498		$<2\times10^{-16}$*		0.348749
A	C	D	Full	0.9704	−0.47646	0.81053	0.08656	0.000261*	0.315632	
A	C	D	Reduced	0.9702	−0.32616	0.97482		2.72×10^{-12}*		0.288321
A	D	B	Full	0.9867	−0.09045	1.28025	−0.44079	8.33×10^{-08}*	0.0767	
A	D	B	Reduced	0.9842	0.32862	1.05801		3.25×10^{-14}*		0.054032
B	A	C	Full	0.998	−0.15579	0.96549	0.09406	$<2\times10^{-16}$*	0.1136	
B	A	C	Reduced	0.9978	−0.24148	1.01282		$<2\times10^{-16}$*		0.110554
B	C	A	Full	0.9907	−0.5037	1.03925	−0.03545	$<2\times10^{-16}$*	0.328	
B	C	A	Reduced	0.9907	−0.56147	1.06752		$<2\times10^{-16}$*		0.002836*
B	D	C	Full	0.9944	0.13957	0.92174	−0.07558	4.93×10^{-16}*	0.0656	
B	D	C	Reduced	0.9936	0.01857	0.99161		$<2\times10^{-16}$*		0.31286
B	D	A	Full	0.9605	0.3037	1.2595	−0.1222	3.42×10^{-05}*	0.273	
B	D	A	Reduced	0.9596	0.09045	1.03398		2.29×10^{-11}*		0.272114
C	A	D	Full	0.9704	0.47646	0.89709	−0.08656	1.17×10^{-7}*	0.31563	
C	A	D	Reduced	0.9702	0.32616	0.97482		2.72×10^{-12}*		0.288321
C	A	B	Full	0.994	0.29497	1.02598	−0.05029	3.03×10^{-15}*	0.0628	
C	A	B	Reduced	0.9932	0.21309	0.9365		$<2\times10^{-16}$*		0.000451*
C	B	A	Full	0.9904	0.49292	0.9889	0.04198	4.60×10^{-12}*	0.256	
C	B	A	Reduced	0.9902	0.56134	1.06435		$<2\times10^{-16}$*		0.004604*
D	B	A	Full	0.9557	−0.2843	1.1266	0.1137	1.94×10^{-7}*	0.339	
D	B	A	Reduced	0.9558	−0.08543	1.02934		4.35×10^{-11}*		0.307599
D	B	C	Full	0.9944	−0.13957	0.84615	0.07558	5.46×10^{-10}*	0.0656	
D	B	C	Reduced	0.9936	−0.01857	0.99161		$<2\times10^{-16}$*		0.31286
Strain combinations with significant influence of the additional strain										
A	B	D	Full	0.9936	−0.4149	1.41257	0.31415	2.36×10^{-13}*	1.48×10^{-5}*	
A	B	D	Reduced	0.9734	0.14543	1.13845		1.22×10^{-12}*		0.048513*
A	C	B	Full	0.9941	−0.30762	0.98947	0.05586	$<2\times10^{-16}$*	0.0411*	
A	C	B	Reduced	0.993	−0.21668	0.94594		$<2\times10^{-16}$*		0.002072*
A	D	C	Full	0.9403	−0.23	0.2308	0.27109	0.2351	0.0161*	
A	D	C	Reduced	0.912	0.21816	0.7259		5.47×10^{-9}*		5.146902×10^{-5}*
B[a]	A	D	Full	0.9934	0.35217	1.63712	−0.28388	9.12×10^{-11}*	0.0000314*	
B	A	D	Reduced	0.9755	−0.1521	1.11188		6.91×10^{-13}*		0.01108461*
B[a]	C	D	Full	0.9948	−1.1418	1.0701	−0.4058	3.8×10^{-13}*	0.0042*	
B	C	D	Reduced	0.9925	−0.80358	0.86603		$<2\times10^{-16}$*		1.432868×10^{-8}*
C	B	D	Full	0.9948	1.1418	0.66435	0.40581	1.62×10^{-9}*	0.0042*	
C	B	D	Reduced	0.9925	0.80358	0.86603		$<2\times10^{-16}$*		1.432868×10^{-8}*
C	D	B	Full	0.9752	1.28137	0.58876	−0.14841	5.25×10^{-09}*	0.0253*	
C	D	B	Reduced	0.9695	1.0455	0.72285		$<2\times10^{-16}$*		4.67659×10^{-10}*
C	D	A	Full	0.9973	0.24646	1.16818	−0.57973	1.47×10^{-12}*	1.29×10^{-05}*	
C	D	A	Reduced	0.9888	0.77397	0.87185		2.84×10^{-15}*		1.119510×10^{-5}*
D[a]	A	B	Full	0.9861	0.1718	0.7963	0.5382	0.0000181*	0.0379*	
D	A	B	Reduced	0.9818	−0.34213	1.06598		8.54×10^{-14}*		0.045915*
D	A	C	Full	0.9403	0.23	0.50189	−0.27109	0.000135*	0.01609*	
D	A	C	Reduced	0.912	−0.21816	0.7259		5.47×10^{-09}*		5.146902×10^{-5}*
D[a]	C	B	Full	0.9752	−1.28137	0.44035	0.14841	0.00146*	0.02528*	

Table 2 (continued)

Target strain	Reference strain	Additional strain	Model	R^2	Intercept β_0	Slopes		p (slopes=0)		p (slope=1)
						β_1	β_2	β_1	β_2	
D	C	B	Reduced	0.9695	−1.0455	0.72285		$<2\times10^{-16}$*		4.67659×10^{-10}*
D	C	A	Full	0.9973	−0.24646	0.58845	0.57973	4.72×10^{-09}*	1.29×10^{-05}*	
D	C	A	Reduced	0.9888	−0.77397	0.87185		2.84×10^{-15}*		1.119510×10^{-5}*

Coefficients and p values resulting from both the full (Eqs. 1 and 2) and the reduced regression models (Eqs. 3 and 4) for each possible combination of strains. α=0.05 was used as significance level

*$p\leq\alpha$

[a] Combination of target and additional strain for which no calibration curves could be established

behaved similarly under the used experimental conditions and, therefore, comparability of biomass estimates is given.

Furthermore, the addition of high amounts of reference mycelium to low amounts of target mycelium can cause biomass estimates to be less accurate. The closer the reference/target weight ratio is to 1, the more accurate estimation of the target's biomass, i.e., the narrower the prediction interval (Fig. 1). However, the lowest amount of powdery freeze-dried mycelium that can accurately be weighed manually, i.e., without the aid of a micromanipulator, is 3 mg. Thus, the reference mycelium weighs 3 mg, which is usually much more than the weight of endophytic mycelium in plant tissues (Fig. 3). Consequently, the reference/target weight ratio is strongly skewed towards values >>1, possibly leading to a bias in quantification of low amounts of target mycelium [30]. To avoid this bias, DNA extraction from a multiple of 21 root pieces would be

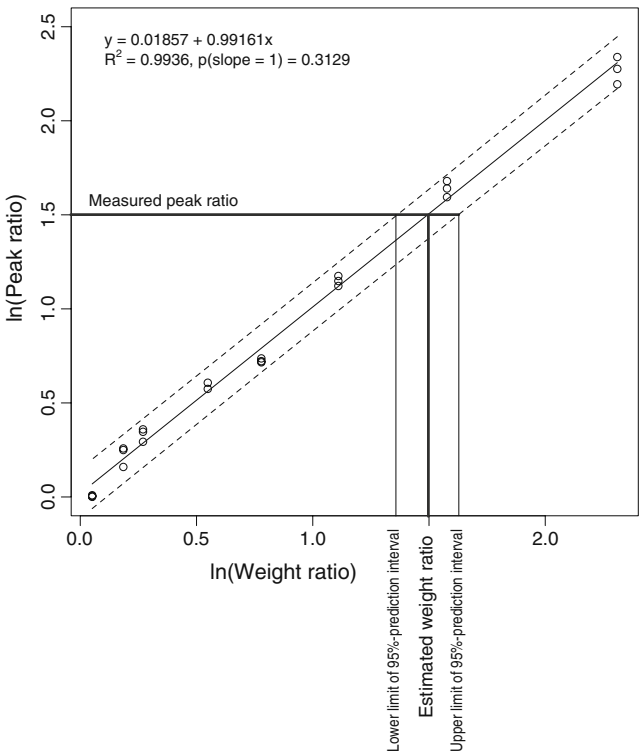

Figure 1 Calibration curve at locus mPF_142B created by competitive microsatellite PCR of DNA extracted from freeze-dried mycelium of strains B (target strain), D (reference strain), and C (additional strain) mixed at different weight ratios. Triplicates of the PCR products were prepared for fragment analysis. The logarithmic ratios of the amount of PCR products (i.e., peak ratios) ($y = p_D/p_B$) were plotted against the logarithmic mycelial weight ratios ($x = m_D/m_B$). The *solid line* represents the regression line fitted to the data points and the *dashed lines* the 95%-prediction interval. The equation of the regression line, the coefficient of determination, the probability of the slope (β_1) being 1, and estimation of the mycelial weight ratio with 95% prediction interval for a supposed peak ratio of 1.5 are also displayed

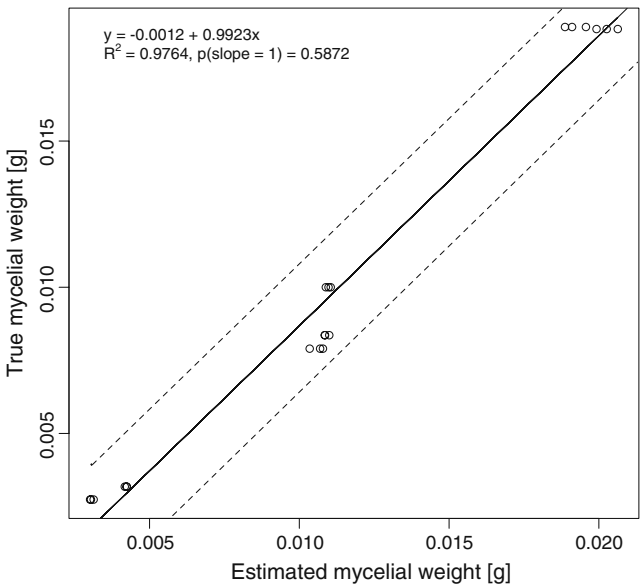

Figure 2 Test for the suitability of calibration curves. True versus estimated mycelial weight of strain A. The calibration curve described on the first line of Table 2 was used to estimate the mycelial weight based on the amount of DNA received by competitive PCR amplification of microsatellite locus mPF_142B. The *dashed lines* indicate the 95% prediction interval. The slope of the regression line does not deviate significantly from 1 (p=0.5872)

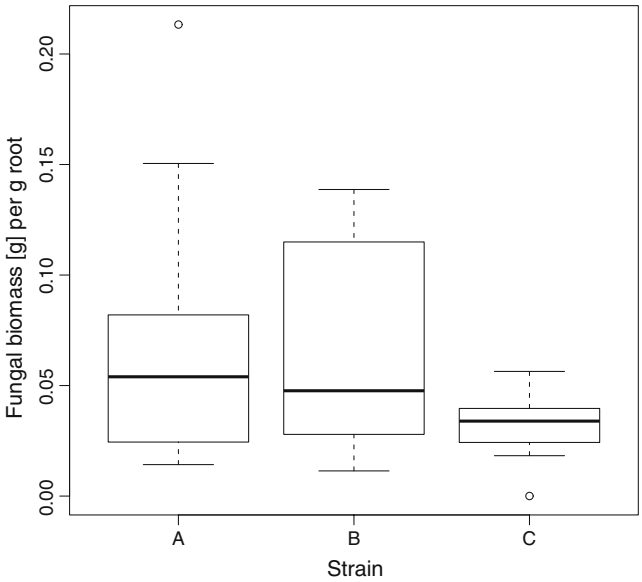

Figure 3 Boxplots depicting the variation of endophytic biomass accumulation of three PAC strains in Norway spruce seedling roots after 4 month of inoculation in a phytotron [16 h day (120–140 $\mu Em^{-2}\ s^{-1}$)/8 h night rhythm, temperature (22°C/15°C), and relative humidity (RH 45%)]

a solution. Additionally, taking more samples from the same root system increases accuracy of the weight-ratio estimates of the two strains colonizing the same root system.

Although real-time quantitative PCR and the microsatellite method were applied to the same DNA extracts, some of the fungal biomass estimates obtained by the two methods deviated strongly from each other (Fig. 4). This is mainly due to the wide confidence intervals of the estimates observed with either method [28]. For example, if the estimates obtained by the two methods for the same extract deviate from the true value in opposite directions, the difference between the two estimates can become very large. An important advantage of the microsatellite method is the presence of a known amount of mycelium of a reference strain as internal standard in each reaction tube during PCR. The amount of light emitted by the reference strain during detection is proportional to the light emitted by the target strain(s). This allows more accurate estimation of the target strains biomass. In contrast, in real-time quantitative PCR, the standard runs separately in a different reaction tube. Therefore, disturbing effects (e.g., substances inhibiting PCR) may affect targets and standard differently. This could lead to larger deviations between estimates and true values compared to the deviations obtained with the microsatellite method. Additionally, the real-time quantitative PCR method consists of two PCRs, a pre-PCR with 15 amplification cycles and the real-time quantitative PCR itself, whereas for the microsatellite method, only one PCR with 36 amplification cycles is needed. Thus, although the initial DNA amount is the same for both methods, the DNA amount after PCR differs between the two methods. Since each PCR run adds some variation, nested real-time quantitative PCR probably generates more variation than the microsatellite method. For all these reasons, we consider the microsatellite method to provide more accurate estimates of endophytic fungal biomass than real-time quantitative PCR. Similarly, Naef et al. [13] found that competitive PCR based on microsatellite sequences is more accurate than the real-time quantitative PCR method. Comparing our method with that of Naef et al. [13], we benefit from the highly polymorphic microsatellites allowing us to distinguish not only among species but also among conspecific strains. The extension of the dual to the triple system may be useful for those working with fungal communities.

The newly developed method offers the possibility to study colonization of roots inoculated with known PAC strains. Not only detection and differentiation of PAC strains are possible but also quantification. On average and depending on the PAC species, approximately 3–6% of the root biomass consisted of mycelial biomass of either one of the two inoculated PAC strains (Fig. 3). In the future, this method can become very useful to study dynamics and performance of PAC strains inoculated into plant communities in natural habitats. Because of possible extension to a multidimensional system, the application spectrum will increase.

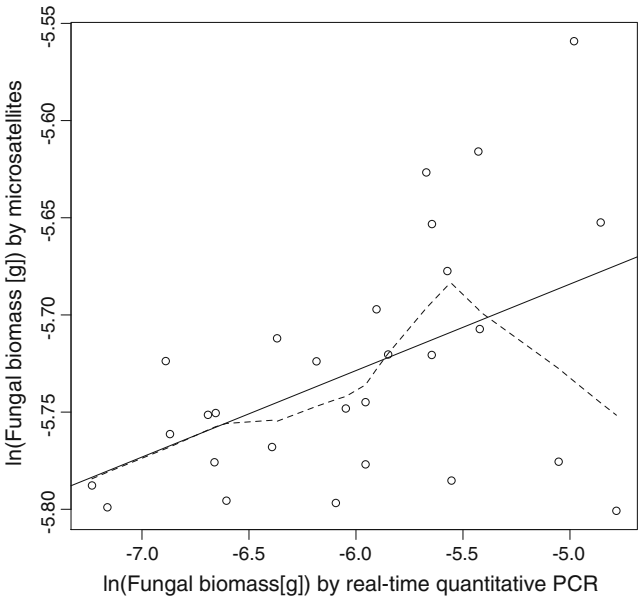

Figure 4 Regression of the estimates of endophytic fungal biomass obtained by the microsatellite method on those obtained by real-time quantitative PCR. The *solid line* indicates linear fit; the *dashed line* indicates LOESS fit with α=0.5

Acknowledgments We would like to thank the Genetic Diversity Centre (GDC) of ETH Zurich for providing the necessary laboratory facilities to perform real-time quantitative PCR and microsatellite analyses. We also thank Manuel Koller of the Seminar for Statistics (SfS), ETH Zurich, for his support. The study represents part of the research project GEDIHAP funded by the Competence Center Environment and Sustainability (CCES) of the ETH Domain.

References

1. Ahlich K, Sieber TN (1996) The profusion of dark septate endophytic fungi in non-ectomycorrhizal fine roots of forest trees and shrubs. New Phytol 132:259–270
2. Atkins SD, Peteira B, Clark IM, Kerry BR, Hirsch PR (2009) Use of real-time quantitative PCR to investigate root and gall colonisation by co-inoculated isolates of the nematophagous fungus *Pochonia chlamydosporia*. Ann Appl Biol 155:143–152
3. Bibby K, Viau E, Peccia J (2010) Pyrosequencing of the 16S rRNA gene to reveal bacterial pathogen diversity in biosolids. Water Res 44:4252–4260
4. Cleveland WS, Devlin SJ (1988) Locally weighted regression—an approach to regression-analysis by local fitting. J Am Stat Assoc 83:596–610
5. Crawley MJ (2007) The R book. Wiley, Chichester
6. Currah RS, Tsuneda A, Murakami S (1993) Morphology and ecology of *Phialocephala fortinii* in roots of *rhododendron brachycarpum*. Can J Bot 71:1639–1644
7. Grünig CR, Linde CC, Sieber TN, Rogers SO (2003) Development of single-copy RFLP markers for population genetic studies of *Phialocephala fortinii* and closely related taxa. Mycol Res 107:1332–1341
8. Grünig CR, Brunner PC, Duo A, Sieber TN (2007) Suitability of methods for species recognition in the *Phialocephala fortinii-Acephala applanata* species complex using DNA analysis. Fungal Genet Biol 44:773–788
9. Grünig CR, Queloz V, Sieber TN, Holdenrieder O (2008) Dark septate endophytes (DSE) of the *Phialocephala fortinii* s.l.—*Acephala applanata* species complex in tree roots: classification, population biology, and ecology. Botany 86:1355–1369
10. Holdenrieder O, Sieber TN (1992) Fungal associations of serially washed healthy nonmycorrhizal roots of *Picea abies*. Mycol Res 96:151–156
11. Jumpponen A, Trappe JM (1998) Dark septate endophytes: a review of facultative biotrophic root-colonizing fungi. New Phytol 140:295–310
12. Melin E (1923) Experimentelle Untersuchungen über die Konstitution und Ökologie der Mykorrhizen von *Pinus sylvestris* L. und *Picea abies* (L.) Karst. In: Falck R (ed) Mykologische Untersuchungen und Berichte 2., pp 73–334
13. Naef A, Senatore M, Defago G (2006) A microsatellite based method for quantification of fungi in decomposing plant material elucidates the role of *Fusarium graminearum* DON production in the saprophytic competition with *Trichoderma atroviride* in maize tissue microcosms. FEMS Microbiol Ecol 55:211–220
14. Queloz V, Grünig CR, Sieber TN, Holdenrieder O (2005) Monitoring the spatial and temporal dynamics of a community of the tree-root endophyte *Phialocephala fortinii* s.l. New Phytol 168:651–660
15. Queloz V, Duo A, Grünig CR (2008) Isolation and characterization of microsatellite markers for the tree-root endophytes *Phialocephala subalpina* and *Phialocephala fortinii* s.s. Mol Ecol Resour 8:1322–1325
16. Queloz V, Duo A, Sieber TN, Grünig CR (2010) Microsatellite size homoplasies and null alleles do not affect species diagnosis and population genetic analysis in a fungal species complex. Mol Ecol Resour 10:348–367
17. R Development Core Team (2010) R: a language and environment for statistical computing. R Foundation for Statistical Computing, Vienna
18. Read DJ, Haselwandter K (1981) Observations on the mycorrhizal status of some alpine plant-communities. New Phytol 88:341–352
19. Schulz B, Boyle C (2005) The endophytic continuum. Mycol Res 109:661–686
20. Sieber TN (2002) Fungal root endophytes. In: Waisel Y, Eshel A, Kafkafi U (eds) Plant roots, the hidden half. Basel, New York, pp 887–917
21. Sieber TN, Grünig CR (2006) Biodiversity of fungal root-endophyte communites and populations, in particular of the dark septate endophyte *Phialocephala fortinii* s.l. In: Schulz B, Boyle C, Sieber T (eds) Microbial root endophytes, vol 9. Springer, Berlin, pp 107–132
22. Sieber TN (2007) Endophytic fungi in forest trees: are they mutualists? Fungal Biol Rev 21:75–89
23. Stoyke G, Egger KN, Currah RS (1992) Characterization of sterile endophytic fungi from the mycorrhizae of sub-alpine plants. Can J Bot 70:2009–2016
24. Summerbell RC (2005) Root endophyte and mycorrhizosphere fungi of black spruce, *Picea mariana*, in a boreal forest habitat: influence of site factors on fungal distributions. Stud Mycol 53:121–145
25. Tedersoo L, Nilsson RH, Abarenkov K, Jairus T, Sadam A, Saar I, Bahram M, Bechem E, Chuyong G, Koljalg U (2010) 454 Pyrosequencing and Sanger sequencing of tropical mycorrhizal fungi provide similar results but reveal substantial methodological biases. New Phytol 188:291–301
26. Tejesvi MV, Mahesh B, Nalini MS, Prakash HS, Kini KR, Subbiah V, Shetty HS (2006) Fungal endophyte assemblages from ethnopharmaceutically important medicinal trees. Can J Microbiol 52:427–435
27. Tejesvi MV, Ruotsalainen AL, Markkola AM, Pirttila AM (2010) Root endophytes along a primary succession gradient in northern Finland. Fungal Divers 41:125–134
28. Tellenbach C, Grünig CR, Sieber TN (2010) Suitability of quantitative real-time PCR to estimate biomass of fungal root endophytes. Appl Environ Microbiol 76:5764–5772
29. Zaffarano PL, Duò A, Grünig CR (2010) Characterization of the mating type (MAT) locus in the *Phialocephala fortinii* s.l.—*Acephala applanata* species complex. Fungal Genet Biol 47:761–772
30. Zentilin L, Giacca M (2007) Competitive PCR for precise nucleic acid quantification. Nat Protoc 2:2092–2104